HHS Public Access

Author manuscript

Arterioscler Thromb Vasc Biol. Author manuscript; available in PMC 2019 January 01.

Published in final edited form as:

Arterioscler Thromb Vasc Biol. 2018 January ; 38(1): 64–75. doi:10.1161/ATVBAHA.117.309907.

Pro-atherogenic flow increases endothelial stiffness via enhanced CD36-mediated oxLDL uptake

Elizabeth LeMaster[1,4], **Ru-Ting Huang**[7], **Chongxu Zhang**[1], **Yedida Bogachkov**[5], **Cassandre Coles**[5], **Tzu-Pin Shentu**[1,4], **Yue Sheng**[3], **Ibra S. Fancher**[1], **Carlos Ng**[4], **Theodore Christoforidis**[4], **Pappasani V. Subbaiah**[2], **Evgeny Berdyshev**[8], **Zhijian Qain**[3], **David T. Eddington**[4], **James Lee**[4], **Michael Cho**[4], **Yun Fang**[7], **Richard D. Minshall**[5,6], and **Irena Levitan**[1,4,5]

[1]Division of Pulmonary and Critical Care, University of Illinois at Chicago

[2]Division of Endocrinology, University of Illinois at Chicago

[3]Division of Hematology and Oncology, Department of Medicine, University of Illinois at Chicago

[4]Department of Bioengineering, University of Illinois at Chicago

[5]Department of Pharmacology, University of Illinois at Chicago

[6]Department of Anesthesiology, University of Illinois at Chicago

[7]Department of Medicine, University of Chicago

[8]National Jewish Health, Denver, Colorado

Abstract

Objective—Disturbed flow (DF) is well-known to induce endothelial dysfunction and synergistically with plasma dyslipidemia facilitate plaque formation. Little is known, however, about the synergistic impact of DF and dyslipidemia on endothelial biomechanics. Our goal was to determine the impact of DF on endothelial stiffness and evaluate the role of dyslipidemia/oxLDL in this process.

Approach and Results—Endothelial elastic modulus of intact mouse aortas *ex vivo* and of human aortic ECs (HAECs) exposed to laminar or disturbed flow was measured using AFM. Endothelial monolayer of the aortic arch (AA) is found to be significantly stiffer than the descending aorta (DA) (4.2+1.1 versus 2.5+0.2 kPa for AA versus DA) in mice maintained on low fat diet (LFD). This effect is significantly exacerbated by short-term high-fat diet (HFD) (8.7+2.5 versus 4.5+1.2 kPa for AA versus DA). Exposure of HAECs to DF *in vitro* resulted in 50% increase in oxLDL uptake and significant endothelial stiffening in the presence but not in the absence of oxLDL. DF also increased the expression of oxLDL receptor CD36 whereas downregulation of CD36 abrogated DF-induced endothelial oxLDL uptake and stiffening. Furthermore, genetic deficiency of CD36 abrogated endothelial stiffening in the aortic arch *in vivo*

Corresponding Author: Irena Levitan, Department of Medicine, University of Illinois at Chicago, 840 South Wood Street, Chicago, IL, 60612-7323, Phone: 312-996-0441, levitan@uic.edu.

Disclosures:
None declared

in mice fed either LFD or HFD. We also show that the loss of endothelial stiffening in CD36 KO aortas is not mediated by the loss of CD36 in circulating cells.

Conclusions—Disturbed flow facilitates endothelial CD36-dependent uptake of oxidized lipids resulting in local increase of endothelial stiffness in pro-atherogenic areas of the aorta.

Keywords

endothelial stiffness; oxLDL; disturbed flow; CD36

Introduction

Atherosclerotic plaques develop preferentially in arterial regions that are exposed to non-unidirectional disturbed flow (DF). The pre-disposition of these regions to atherosclerosis is attributed to the hemodynamic forces that act on the endothelium: unidirectional fluid shear stress in uniform straight vessels is athero-protective whereas the recirculating disturbed low flow at bifurcations is pro-atherogenic[1–3]. Multiple studies showed that exposure to DF induces a variety of pro-inflammatory genes and pathways whereas laminar flow (LF) is anti-inflammatory[2–4]. It is also well-known that while DF alone causes endothelial dysfunction and pre-disposes the region to plaque development it is the combination of DF and dyslipidemia that results in the development of atherosclerotic plaques. Little is known, however, about the mechanisms of the synergistic effects of disturbed flow and dyslipidemia on endothelial properties.

Oxidative modifications of LDL (oxLDL) play a major role in dyslipidemia-induced endothelial dysfunction and the onset of atherosclerosis. Briefly, oxLDL accumulates in atherosclerotic lesions and was found to correlate with cardiovascular events[5, 6]. Furthermore, mouse models of genetic deficiency in endothelial scavenger receptors that recognize oxLDL were shown to have athero-protective effects[7, 8]. OxLDL was also found to be cytotoxic to endothelial cells (ECs), to impair the integrity of the endothelial barrier, impair the production of nitric oxide, increase reactive oxygen species and promote the release of pro-inflammatory cytokines[6, 9, 10]. Our earlier studies showed that exposure to oxLDL results in a significant increase in endothelial stiffness and contractility[11–13]. In terms of the mechanism, we have shown oxLDL-induced endothelial stiffening is mediated by the uptake of oxidized lipids[13, 14,15] and can be fully attributed to the activation of the RhoA/ROCK/MLCP/MLC2 cascade[16]. In the current study, we investigate the regional heterogeneity of endothelial stiffness between the athero-susceptible region of the aortic arch and athero-resistant region of the descending aorta and determine the impact of pro- and anti-atherogenic flow environments on endothelial uptake of oxLDL and EC stiffness.

Methods

Materials and Methods are available in the online-only Data Supplement.

Results

High cholesterol diet results in endothelial stiffening: enhanced effect in athero-susceptible regions of the aorta

The impact of high cholesterol/high fat (HFD) diet on endothelial stiffness *in vivo* in the aortic arch (AA) and the descending aorta (DA) was tested using a mouse model of diet-induced endothelial dysfunction described earlier[17]. Briefly, six week old C57BL/6 male mice were fed HFD for one month resulting in a significant increase in weight gain (15% versus 33%), total cholesterol, LDL and oxLDL (Fig.1A), as compared to mice fed low fat diet (LFD). Notably, although there was a low lipid content in the aortic tissues of LFD-fed mice, as assessed by Oil Red-O staining of histological sections (Fig.1C, with PECAM-1 staining shown in Fig.1B), there was a significant increase in lipid accumulation in the AA as compared to the DA (Fig.1D). Furthermore, we performed liquid chromatography-electrospray ionization tandem mass spectrometric (LC-ESI-MS/MS) analysis of cholesterol and cholesterol esters in the AA and DA tissues from mice on both LFD and HFD (Fig.1E). A small increase in free cholesterol content in the AA regions was observed in 5 out of 8 mice on LFD and in 4 out 4 mice on HFD but it was not statistically significant (Fig.1E, left two panels). We also observed a significant increase in the level of cholesterol esters in the AA regions, which was exacerbated by a HFD (Fig.1E, right two panels).

Endothelial stiffness was evaluated by measuring the elastic modulus of the endothelial monolayer of intact arteries using atomic force microscopy (AFM). For all animals, the stiffness of the endothelium was measured in the DA and AA regions (6–10 distinct sites measured for each region for each animal, micro-indentation depth of 0.5–1μm, 10–15% of the cell height). The integrity of the endothelial monolayer was confirmed by *en face* staining with an endothelial marker, PECAM-1, showing the characteristic endothelial morphology in the DA and AA regions (Fig.1F). First, we compared the elastic moduli of the endothelium of DA and AA regions of aortas isolated from mice maintained on LFD (Fig.1G, top row). These data show that the endothelium of the AA region has a higher elastic modulus (increased stiffness) as compared to the endothelium of the DA, as represented by the rightward shift in the histogram. Average elastic moduli for DA and AA regions for each mouse in this experimental group are shown in Fig.1H. Introducing HFD resulted in significant stiffening of the endothelium in both the DA and AA regions, with the effect clearly enhanced in the AA region (Fig.1G bottom row, Fig.1H). All mice were gender and age-matched and experiments on LFD and HFD-fed mice were performed in parallel.

Differential effects of laminar and disturbed flow on oxLDL-induced endothelial stiffening

Since our previous studies showed that endothelial stiffness is significantly increased in cells exposed to oxLDL[11–13] and since it was recently shown that oscillatory flow results in increased oxLDL uptake in coronary ECs[18], we hypothesized that an increase in endothelial stiffness in the arch regions of the aortas may be mediated by enhanced oxLDL uptake and oxLDL-induced endothelial stiffening. To test this hypothesis, we compared oxLDL uptake in human aortic endothelial cells (HAECs) exposed to laminar unidirectional flow versus non-unidirectional disturbed flow using a microfluidic flow chamber with a step barrier (Suppl.Fig.IA, Fig.2A), a modification of a step-barrier flow chamber described earlier.[19]

Using computational fluid dynamics (CFD) analysis, it was determined that for the specific parameters of the step width and height, the device created a recirculation region of 2 mm after the step (Suppl.Fig.IB). The validity of this design was verified by imaging the trajectories of fluorescent beads in recirculating and laminar regions of the chamber (Suppl.Fig. IA[d]) and EC alignment (Suppl.Fig. IC).

Our results show that oxLDL uptake in HAECs exposed to DF was significantly higher than in cells exposed to LF (Fig.2B,C). Uptake of DiI-oxLDL (1 μg/mL) was measured in HAECs grown in 0.2% gelatin-coated microfluidics devices, in cells exposed to 10–12 dyn/cm^2 of laminar/uni-directional or <3 dyn/cm^2 recirculating/disturbed flow for 48 hours, by quantifying the oxLDL-specific fluorescence. The oxLDL concentration used for uptake experiments is based on the reported range of oxLDL in human plasma (from 0.2–0.4 to 7–31 μg/mL, K_D of oxLDL binding to CD36 ~3–7 μg/mL at 4°C)[20]. No increase in fluorescence was observed in the absence of DiI-oxLDL (Suppl.Fig.IIA) and DiI-oxLDL fluorescence was blocked by non-fluorescent oxLDL verifying the specificity of the DiI-oxLDL fluorescent signal (Suppl.Fig.IIB). In all uptake experiments, DiI-oxLDL fluorescence was quantified after removing oxLDL particles from the cell surface using an acid wash (Suppl.Fig.IIC). Concentration-dependent DiI-oxLDL fluorescent signal did not saturate at the concentrations used in these experiments (Suppl.Fig.IID). A similar behavior was observed for DiI-LDL (Suppl.Fig.IIE).

An increase in oxLDL uptake was also observed in HAECs exposed for 48 hours to pro-atherogenic DF, as compared to athero-protective LF waveforms created by a cone and plate apparatus that generates physiologically-relevant shear stress patterns (e.g.[21]) (Fig.2D,E,F). Furthermore, we performed LC-ESI-MS/MS analysis of cholesterol and oxysterol contents in HAECs exposed to athero-protective versus pro-atherogenic flows. This analysis shows that while no significant increase was observed in cholesterol content (Fig.2G, inset), there was a significant increase in the level of several oxysterols: 7-ketocholesterol, 5α,6α-epoxycholestanol and 27-OH-cholesterol (Fig.2G).

Increased oxLDL uptake in the DF regions resulted in a significant increase in endothelial stiffness (Fig.2H,I). The elastic modulus was measured following 48 hours exposure to flow in the presence or absence of 10 μg/mL oxLDL in the medium. The upper panel of the chamber was removed after the cessation of flow to allow the AFM tip access to the cell surface. Regions exposed to laminar versus disturbed flow were identified by the proximity to the barrier. No difference in the elastic modulus of HAECs was observed in DF versus LF regions in the absence of oxLDL (Fig.2H,I). We also observed that oxLDL-induced HAECs stiffening was dose-dependent under static conditions (Suppl.Fig.III). Also, independent experiments showed that while cells grown and flow-treated on a collagen substrate are stiffer overall than those on a gelatin or fibronectin substrate, there was no difference in the cellular elastic modulus between DF versus LF regions in each condition in the absence of oxLDL (Suppl.Fig.IV).

OxLDL-induced endothelial stiffening under disturbed flow is mediated by increased expression of CD36

To elucidate the mechanism of increased oxLDL uptake and endothelial stiffening under disturbed flow conditions, we first tested the impact of differential flow patterns on the mRNA expression of two major endothelial oxLDL receptors, CD36 and Lox1. Both CD36 and Lox1 are expressed in HAECs and mRNA expression of both increased in response to pro-atherogenic flow as compared to athero-protective flow (Fig.3A). Notably, the level of CD36 mRNA expression was 70-fold higher than Lox1. Also, as we showed previously[16], CD36 is expressed in HAECs on the protein level (Fig.3B) but is lower than in human microvascular ECs (Suppl.Fig.V). Moreover, protein expression of CD36 is higher in cells exposed to disturbed flow (P-A) when compared to cells exposed to laminar flow (A-P in Fig.3B, negative and positive controls of CD36 expression in CHO cells are shown in Suppl.Fig.V). In addition, Fig.3B shows no difference in CD36 expression between the static condition and either of the flow conditions, which is also observed on the mRNA level as well (data not shown). No significant effect between the static and the flow conditions was observed for Lox1 mRNA (data not shown) and protein (Suppl.Fig.VI) expression levels. Furthermore, expression of CD36 on the plasma membrane of HAECs was confirmed by immunostaining and z-stack confocal imaging in non-permeabilized cells labeled with a plasma membrane marker (Fig.3C) and by TIRF microscopy which showed CD36 on the membrane (Fig.3D, left: TIRF, right: epifluorescence). Protein expression of CD36 was also significantly increased in DF, as determined by immunostaining HAECs exposed to flow in the step barrier chamber in the presence of oxLDL (Fig.3E,F). The specificity of the CD36 fluorescence was verified using CD36-targeting siRNAs demonstrating that downregulation of the protein dramatically decreased the signal. The knock-down effect was verified by qPCR and by Western Blot analysis (Suppl.Fig.VII).

Our further studies show that oxLDL uptake by HAECs is mediated by CD36. Cell surface binding and internalization of DiI-oxLDL is dependent on CD36 expression as evidenced by reduced DiI-oxLDL in HAECs treated with CD36-targeting siRNA (Fig.4A,B). Next, we assessed the role of CD36 in the disturbed flow induced increase in oxLDL uptake. The downregulation of CD36 (using two different CD36-targeting siRNAs) significantly decreased the uptake of oxLDL under both laminar and recirculating/disturbed flow and abrogated the increase in oxLDL uptake in response to DF (Fig.4C,D). Downregulation of CD36 expression also abrogated oxLDL-induced endothelial stiffening both under LF and DF and eliminated the differential effect between the two flow environments on endothelial stiffness (Fig.4E,F). No change in endothelial elastic modulus was observed between laminar and disturbed flow in the absence of oxLDL (Fig.4F). Also, downregulation of CD36 had no effect on endothelial stiffness in cells not exposed to oxLDL. In contrast, downregulation of Lox1 expression had no effect on oxLDL uptake, leaving the effect of DF fully preserved (Suppl.Fig.VIII).

Endothelial stiffening in the aortic arch critically depends on CD36 expression

Next, we applied mechanistic insights gleaned from our current studies investigating DF/oxLDL-induced endothelial stiffening *in vitro* to elucidate the mechanism of endothelial stiffening in athero-susceptible aortic regions *in vivo*.

To determine a potential contribution of the oxLDL/CD36 pathway to EC stiffening, we utilized the mouse model that is globally deficient in the CD36 receptor. Initially studies in WT mice showed a small but significant increase in CD36 expression in the AA versus DA regions, as determined by immunostaining of the histological sections (Fig.5A,B). Immunohistological staining of CD36 was confirmed by significantly reduced staining in the histological sections of the aortic tissues isolated from CD36 KO mice compared to the WT mice (Suppl.Fig.IX). Also, while there was an increase in lipid depositions in the arch in CD36KO mice (0.3±0.1% area in DA and 0.9±0.1% area in AA), the level of the lipid deposition in general was significantly lower than in the WT tissues (1.2±0.1% area versus 2.5±0.1% area in DA and AA, respectively). In the first series of experiments, aortas were isolated from WT and CD36 KO age-matched male mice maintained on LF diet (5–6 months old). Similar to the effect observed in younger mice described above, there was significant endothelial stiffening in the AA versus DA in WT mice (Fig.5C,D). In contrast, no stiffening was observed in the endothelium of the arch regions in CD36 KO mice (Fig. 5C,D). Furthermore, a separate cohort of 2 month old CD36 KO mice were fed HF diet or maintained on LF diet for one month, the same regiment used in WT mice described above. Similarly to WT mice, CD36 KO mice gained significant amount of weight when fed HFD and had elevated levels of oxLDL in the plasma (Fig. 5E). However, in contrast to WT mice, no difference in endothelial elastic modulus was observed between AA and DA regions in CD36 KO mice maintained both on LFD or HFD (Fig.5F). Interestingly, the range of endothelial elastic moduli in CD36 KO mice on both LF and HF diets was similar to the DA region in WT mice on LFD, despite a similar increase in body weight and plasma oxLDL concentrations.

Finally, to exclude the possibility that the decrease in endothelial stiffening in CD36 KO mice could be due to a “trans” effect of the loss of CD36 in circulating cells, we performed a bone marrow transplant study in which wild type marrow was transplanted into CD36 KO mice. Briefly, we harvested bone marrow from WT mice expressing a Ly5.1 marker to identify the donor cells after the implantation, isolated the monocytes and injected them into irradiated WT and CD36 KO mice. The percent incorporation of WT donor macrophages, one month post transplantation, was over 95% for the recipient WT and CD36 KO mice (Fig.6A). Elastic modulus measurements of endothelial monolayers of the recipient WT mice continued to show an increased stiffening effect in the AA as compared to the DA. In comparison, endothelial elastic modulus values from both the DA and the AA from CD36 KO mice were low despite successful incorporation of donor WT macrophages (Fig.6B,C). This shows that the relative softening seen in CD36 KO mice is not a “trans” effect of CD36 loss in circulating cells.

Discussion

This study shows that pro-atherogenic disturbed flow induces endothelial stiffening by facilitating endothelial uptake of oxLDL via CD36 scavenger receptor, and demonstrates a novel mechanism of synergistic interaction between pro-atherogenic flow and dyslipidemia that alters the endothelial biomechanical phenotype in athero-susceptible regions of the aorta.

An increase in vascular stiffness is associated with aging and cardiovascular disease[22]. Our study, however, is focused not on the stiffness of the vascular wall, dominated by extracellular matrix and layers of smooth muscle cells, but on stiffness of the endothelial monolayer, which by itself can be a major factor in regulating barrier function and adhesion and transmigration of immune cells[23, 24]. To test the effects of dyslipidemia, we used a mouse model of diet-induced obesity in WT mice, known to induce endothelial dysfunction and considered to have translational impact when compared to human obesity[17, 25]. Our findings demonstrate that short-term plasma dyslipidemia is sufficient to induce significant *endothelial* stiffening of intact aortas and strongly exacerbate endothelial stiffening in aortic arch observed in animals on low fat diet.

Currently, there is only scarce information about endothelial stiffness in intact arteries. A recent study by Collins *et al.* showed increased endothelial response to force in the AA as compared to the DA in WT mice, an effect that was attributed to increased fibronectin depositions[26]. Our data is in agreement with this study in terms of increased endothelial stiffness in the arch. We provide evidence, however, that this effect is mediated by increased endothelial uptake of oxidized lipids. First, it is abrogated by genetic deficiency of a scavenger receptor CD36 and exacerbated by plasma dyslipidemia, also in CD36-dependent way. It is also supported by our observations *in vitro* that oxLDL is required for the DF-induced stiffening. Notably, elastic modulus measured in our study reflects endothelial deformability/stiffness without additional intervention whereas previous study measured the stiffening response to a local application of force via microbeads, a significantly different parameter, which could be mediated by a different mechanism. Both parameters may have significant physiological consequences.

The well-documented effects of substrate stiffness on endothelial responses[27] and biomechanical properties[28], also raise a possibility that endothelial stiffening in aortic arch could be an indirect result of stiffening of the vascular wall. However, while we cannot fully exclude this possibility, our *in vitro* data indicates that endothelial stiffening develops as a result of DF-induced increase in oxLDL uptake in the absence of any changes in the substrate stiffness. Together with demonstrating lipid accumulation in the aortic arch even in the low fat diet and the abrogation of the stiffening effect by CD36 deficiency, our data suggest that it is the lipid uptake that is responsible for endothelial stiffening.

Another important finding is that exposure to disturbed flow *per se* created as a region of recirculation does not induce endothelial stiffening as compared to laminar flow in the same flow channel, which does not contradict previous studies showing that exposure to LF results in endothelial stiffening as compared to static environment[29]. These observations underscore the importance of comparing different physiologically-relevant flow patterns in the analysis of the effect of flow on endothelial biomechanics.

In terms of the mechanism of oxLDL uptake by aortic endothelium, our data show that an increase in oxLDL uptake under disturbed flow results from increased expression of CD36 whereas Lox1, plays no detectable role. Consistently, we have recently shown that it is CD36 and not Lox1 that is required for oxLDL-induced endothelial stiffening under static conditions[13]. It was initially surprising because most previous studies focused on Lox1 as

the primary oxLDL receptor in ECs[10, 30] but the current study fully support our previous findings. Moreover, an increase in CD36 expression in response to DF, which results in enhanced oxLDL uptake and stiffening, suggests that it can contribute to endothelial dysfunction in disturbed flow. This conclusion is further supported by the *in vivo* observations showing that CD36 deficiency prevents endothelial stiffening in dyslipidemia.

The next major question is to determine the mechanistic link between the binding of oxLDL to CD36, oxLDL internalization and activation of the RhoA/ROCK/MLCP/MLC2 cascade, which we have recently shown to induce endothelial stiffening[16]. Our most recent study suggests that oxLDL induces RhoA activation by causing its dissociation from the RhoA inhibitory protein GDI-1[31], one of the major regulators of RhoA in endothelial cells[32, 33]. Furthermore, since it is known that GDI-1 interacts with RhoA via a hydrophobic pocket and can be displaced by specific lipids, we propose that it is the incorporation of oxidized lipids that is responsible for the dissociation of GDI-1 from RhoA resulting in the activation of RhoA cascade and EC stiffening. In this scenario, the role of CD36 is to mediate internalization of oxLDL leading to the incorporation of oxidized lipids into the membrane. This hypothesis is also consistent with our earlier studies showing that direct incorporation of specific oxysterols, oxidized phospholipids or even cholesterol depletion is sufficient to induced EC stiffening[11–13,15]. However, it is important to note that activation of CD36 may also result in RhoA activation via multiple signaling pathways, including generation of ROS, activation of Src phosphorylation cascades or transactivation of VEGF[34]. Further studies are needed to address these possibilities.

Supplementary Material

Refer to Web version on PubMed Central for supplementary material.

Acknowledgments

We thank Gregory Kowalsky for his assistance with fluorescent imaging and the parallel-plate flow machine and Peter Toth for his help with the TIRF and confocal microscopy experiments.

Sources of Funding:

This study is supported by NIH grants HL-073965 (IL,DE), HL-083298 (IL,RM,MC,PVS), HL-060678 (RM), HL-125356 (RM) and R00 HL-103789 (YF); AHA MWA Pre-doctoral Fellow 14PRE20490156 (EL) and the Chicago Biomedical Consortium with support from the Searle Funds at the Chicago Community Trust (DE).

List of Abbreviations

oxLDL	oxidized low density lipoprotein
DiI-oxLDL-1	1'-dioctadecyl-3,3,3',3'-tetra-methyl-indocarbocyanine perchlorate
LF	laminar flow
DF	disturbed flow
EC	endothelial cells

HAECs	human aortic endothelial cells
MMVECs	mouse microvascular endothelial cells
LFD	low fat diet
HFD	high fat diet
DA	descending aorta
AA	aortic arch
WT	wild type
KO	knockout
ATM	atomic force microscopy

References

1. Hahn C, Schwartz MA. Mechanotransduction in vascular physiology and atherogenesis. Nat Rev Mol Cell Biol. 2009; 10:53–62. [PubMed: 19197332]
2. Tarbell JM, Shi Z-D, Dunn J, Jo H. Fluid Mechanics, Arterial Disease, and Gene Expression. Annual review of fluid mechanics. 2014; 46:591–614.
3. Jiang Y-Z, Manduchi E, Jiménez JM, Davies PF. Endothelial Epigenetics in Biomechanical Stress: Disturbed Flow–Mediated Epigenomic Plasticity In Vivo and In Vitro. Arteriosclerosis, Thrombosis, and Vascular Biology. 2015; 35:1317–1326.
4. Marin T, Gongol B, Chen Z, Woo B, Subramaniam S, Chien S, Shyy JYJ. Mechanosensitive microRNAs—role in endothelial responses to shear stress and redox state. Free Radical Biology and Medicine. 2013; 64:61–68. [PubMed: 23727269]
5. Itabe H, Obama T, Kato R. The Dynamics of Oxidized LDL during Atherogenesis. Journal of Lipids. 2011; 2011:9.
6. Maiolino G, Rossitto G, Caielli P, Bisogni V, Rossi GP, Calo LA. The Role of Oxidized Low-Density Lipoproteins in Atherosclerosis: The Myths and the Facts. Mediators of Inflammation. 2013; 2013:13.
7. Febbraio M, Podrez EA, Smith JD, Hajjar DP, Hazen SL, Hoff HF, Sharma K, Silverstein RL. Targeted disruption of the class B scavenger receptor CD36 protects against atherosclerotic lesion development in mice. The Journal of Clinical Investigation. 2000; 105:1049–1056. [PubMed: 10772649]
8. Mehta JL, Sanada N, Hu CP, et al. Deletion of LOX-1 Reduces Atherogenesis in LDLR Knockout Mice Fed High Cholesterol Diet. Circulation Research. 2007; 100:1634–1642. [PubMed: 17478727]
9. Levitan I, Volkov S, Subbaiah PV. Oxidized LDL: Diversity, patterns of recognition and pathophysiology. Antioxidants & Redox Signaling. 2010; 13:39–75. [PubMed: 19888833]
10. Lubrano V, Balzan S. Lox-1 and ros, inseparable factors in the process of endothelial damage. Free Radical Research. 2014; 48:841–848. [PubMed: 24886290]
11. Byfield FJ, Tikku S, Rothblat GH, Gooch KJ and Levitan I. OxLDL increases endothelial stiffness, force generation and network formation. J Lipid Res. 2006; 47:715–723. [PubMed: 16418538]
12. Shentu TP, Titushkin I, Singh DK, Gooch KJ, Subbaiah PV, Cho M, Levitan I. oxLDL-induced decrease in lipid order of membrane domains is inversely correlated with endothelial stiffness and network formation. Am J Physiol Cell Physiol. 2010; 299:C218–229. [PubMed: 20410437]
13. Shentu TP, Singh DK, Oh M-J, Sun S, Sadaat L, Makino A, Mazzone T, Subbaiah PV, Cho M, Levitan I. The role of oxysterols in control of endothelial stiffness. Journal of Lipid Research. 2012; 53:1348–58. [PubMed: 22496390]

14. Byfield FJ, Aranda-Espinoza H, Romanenko VG, Rothblat GH, Levitan I. Cholesterol depletion increases membrane stiffness of aortic endothelial cells. Biophysical journal. 2004; 87:3336–43. [PubMed: 15347591]
15. Ayee MA, LeMaster E, Shentu TP, Singh DK, Barbera N, Soni D, Tiruppathi C, Subbaiah PV, Berdyshev E, Bronova I, Cho M, Akpa BS, Levitan I. Molecular-Scale Biophysical Modulation of an Endothelial Membrane by Oxidized Phospholipids. Biophysical journal. 2017; 112:325–338. [PubMed: 28122218]
16. Oh MJ, Zhang C, LeMaster E, Adamos C, Berdyshev E, Bogachkov Y, Kohler EE, Baruah J, Fang Y, Schraufnagel DE, Wary KK, Levitan I. Oxidized-LDL Signals through Rho-GTPase to Induce Endothelial Cell Stiffening and Promote Capillary Formation. Journal of lipid research. 2016
17. Collins S, Martin TL, Surwit RS, Robidoux J. Genetic vulnerability to diet-induced obesity in the C57BL/6J mouse: physiological and molecular characteristics. Physiology & Behavior. 2004; 81:243–248. [PubMed: 15159170]
18. Martorell J, Santomá P, Kolandaivelu K, Kolachalama VB, Melgar-Lesmes P, Molins JJ, Garcia L, Edelman ER, Balcells M. Extent of flow recirculation governs expression of atherosclerotic and thrombotic biomarkers in arterial bifurcations. Cardiovascular Research. 2014; 103:37–46. [PubMed: 24841070]
19. DePaola N, Davies PF, Pritchard WF, Florez L, Harbeck N, Polachek DC. Spatial and temporal regulation of gap junction connexin43 in vascular endothelial cells exposed to controlled disturbed flows in vitro. Proc Natl Acad Sci USA. 1999; 96:3154–3159. [PubMed: 10077653]
20. Itabe H, Ueda M. Measurement of plasma oxidized low-density lipoprotein and its clinical implications. Journal of atherosclerosis and thrombosis. 2007; 14:1–11. [PubMed: 17332686]
21. Wu C, Huang R-T, Kuo C-H, et al. Mechanosensitive PPAP2B Regulates Endothelial Responses to Atherorelevant Hemodynamic Forces. Circulation Research. 2015; 117:e41–e53. [PubMed: 26034042]
22. Kohn JC, Lampi MC, Reinhart-King CA. Age-related vascular stiffening: Causes and consequences. Frontiers in Genetics. 2015; 6:112. [PubMed: 25926844]
23. Schaefer A, te Riet J, Ritz K, Hoogenboezem M, Anthony EC, Mul FPJ, de Vries CJ, Daemen MJ, Figdor CG, van Buul JD, Hordijk PL. Actin-binding proteins differentially regulate endothelial cell stiffness, ICAM-1 function and neutrophil transmigration. Journal of Cell Science. 2014; 127:4470–4482. [PubMed: 25107367]
24. Martinelli R, Zeiger AS, Whitfield M, Sciuto TE, Dvorak A, Van Vliet KJ, Greenwood J, Carman CV. Probing the biomechanical contribution of the endothelium to lymphocyte migration: diapedesis by the path of least resistance. Journal of Cell Science. 2014; 127:3720–3734. [PubMed: 25002404]
25. Park Y, Booth FW, Lee S, Laye MJ, Zhang C. Physical activity opposes coronary vascular dysfunction induced during high fat feeding in mice. The Journal of Physiology. 2012; 590:4255–4268. [PubMed: 22674721]
26. Collins C, Osborne LD, Guilluy C, Chen Z, O'Brien ET 3rd, Reader JS, Burridge K, Superfine R, Tzima E. Haemodynamic and extracellular matrix cues regulate the mechanical phenotype and stiffness of aortic endothelial cells. Nature communications. 2014; 5:3984.
27. Kohn JC, Lampi MC, Reinhart-King CA. Age-related vascular stiffening: causes and consequences. Frontiers in genetics. 2015; 6:112. [PubMed: 25926844]
28. Byfield FJ, Reen RK, Shentu T-P, Levitan I, Gooch KJ. Endothelial actin and cell stiffness is modulated by substrate stiffness in 2D and 3D. Journal of Biomechanics. 2009; 42:1114. [PubMed: 19356760]
29. Sato M, Ohashi T. Biorheological views of endothelial cell responses to mechanical stimuli. Biorheology. 2005; 42:421–41. [PubMed: 16369082]
30. Pirillo A, Norata GD, Catapano AL. Lox-1, oxldl, and atherosclerosis. Mediators of Inflammation. 2013
31. Zhang C, Adamos C, Oh MJ, Baruah J, Ayee MAA, Mehta D, Wary KK, Levitan I. oxLDL induces endothelial cell proliferation via Rho/ROCK/Akt/p27kip1 signaling: opposite effects of oxLDL and cholesterol loading. American journal of physiology Cell physiology. 2017; 313:C340–c351. [PubMed: 28701359]

32. Holinstat M, Mehta D, Kozasa T, Minshall RD, Malik AB. Protein kinase Calpha-induced p115RhoGEF phosphorylation signals endothelial cytoskeletal rearrangement. The Journal of biological chemistry. 2003; 278:28793–8. [PubMed: 12754211]

33. Knezevic N, Roy A, Timblin B, Konstantoulaki M, Sharma T, Malik AB, Mehta D. GDI-1 phosphorylation switch at serine 96 induces RhoA activation and increased endothelial permeability. Molecular and cellular biology. 2007; 27:6323–33. [PubMed: 17636025]

34. Silverstein RL, Li W, Park YM, Rahaman SO. Mechanisms of cell signaling by the scavenger receptor CD36: implications in atherosclerosis and thrombosis. Transactions of the American Clinical and Climatological Association. 2010; 121:206–20. [PubMed: 20697562]

Highlights

- Plasma dyslipidemia results in endothelial stiffening of intact aortas and increases the heterogeneity of endothelial elastic moduli between the athero-protective and pro-atherogenic regions.
- Pro-atherogenic disturbed flow induces endothelial stiffening by facilitating endothelial uptake of oxLDL via CD36 pathway.
- Disturbed flow facilitates endothelial CD36-dependent uptake of oxidized lipids resulting in a local increase of endothelial stiffness in the aortic arch.

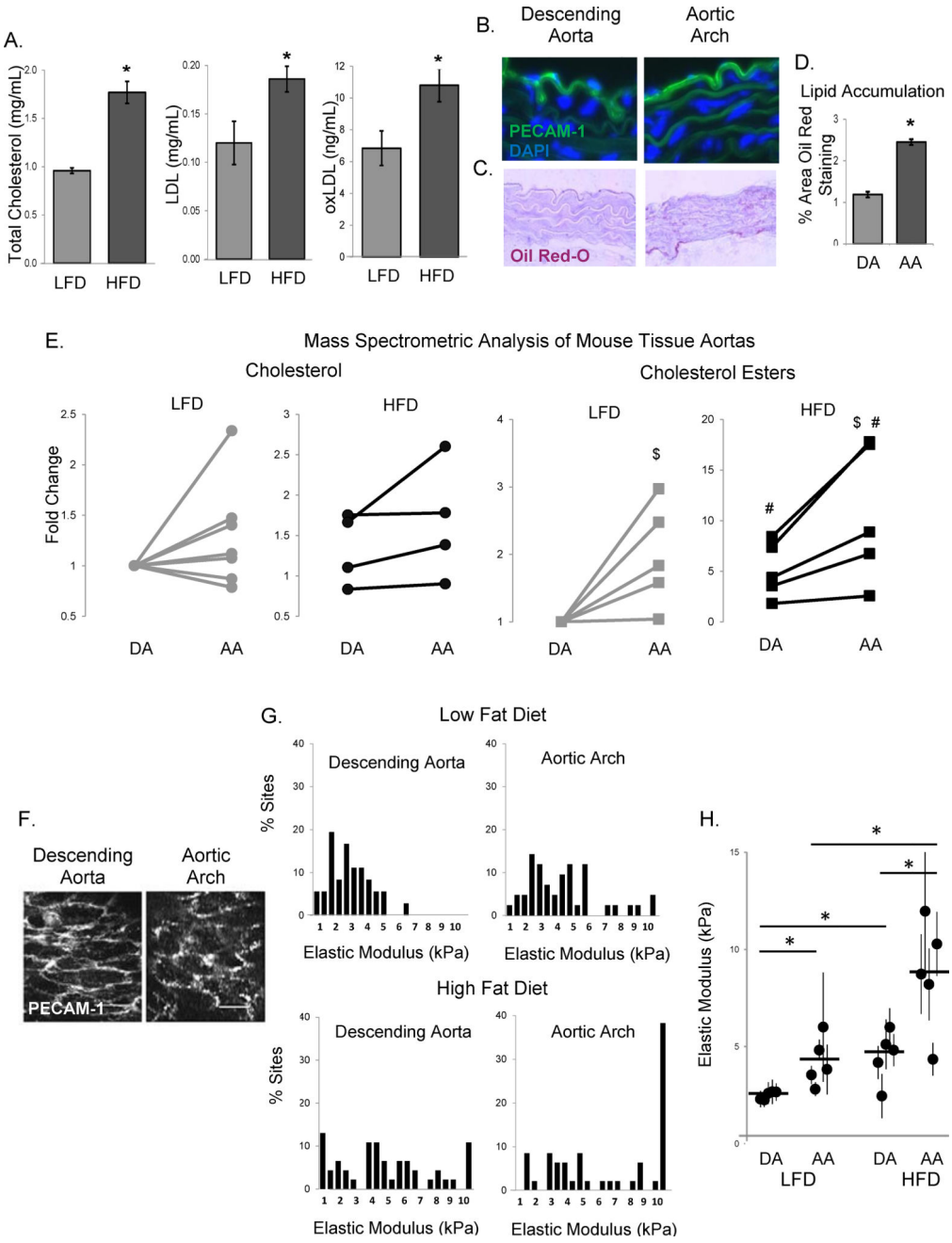

Figure 1. High fat, high cholesterol diet results in aortic endothelial stiffening

A: Total cholesterol, LDL, and oxLDL levels in the plasma of LFD and HFD-fed mice (n=5 mice per group). ***B:*** Typical histological images of staining for PECAM-1 (endothelial marker) in the descending aorta (DA, left) and aortic arch (AA, right). ***C:*** Representative images of sectioned DA (left) and AA (right) stained with Oil Red-O. ***D:*** Average Oil Red-O staining in mouse aortas (n=4, 3–6 sections per mouse). ***E:*** Quantification of the cholesterol (left) and cholesterol ester (right) composition in the descending aorta and aortic arch of LFD or HFD mice (n=4–8 mice) using mass spectrometric analysis. ***F:*** Typical images of *en face* staining for PECAM-1 in the DA (left) and the AA (right). Scale bar=20 microns. ***G:***

Histograms of elastic moduli of the endothelial monolayer of DA and AA freshly harvested from LFD and HFD-fed WT mice (6–10 sites [50–90 measurements] per sample, n=5 mice per condition). ***H:*** Average elastic moduli for the AA and DA regions from each mouse, respectively. $p<0.05 with DA; #p<0.05 with LFD; *p<0.05.

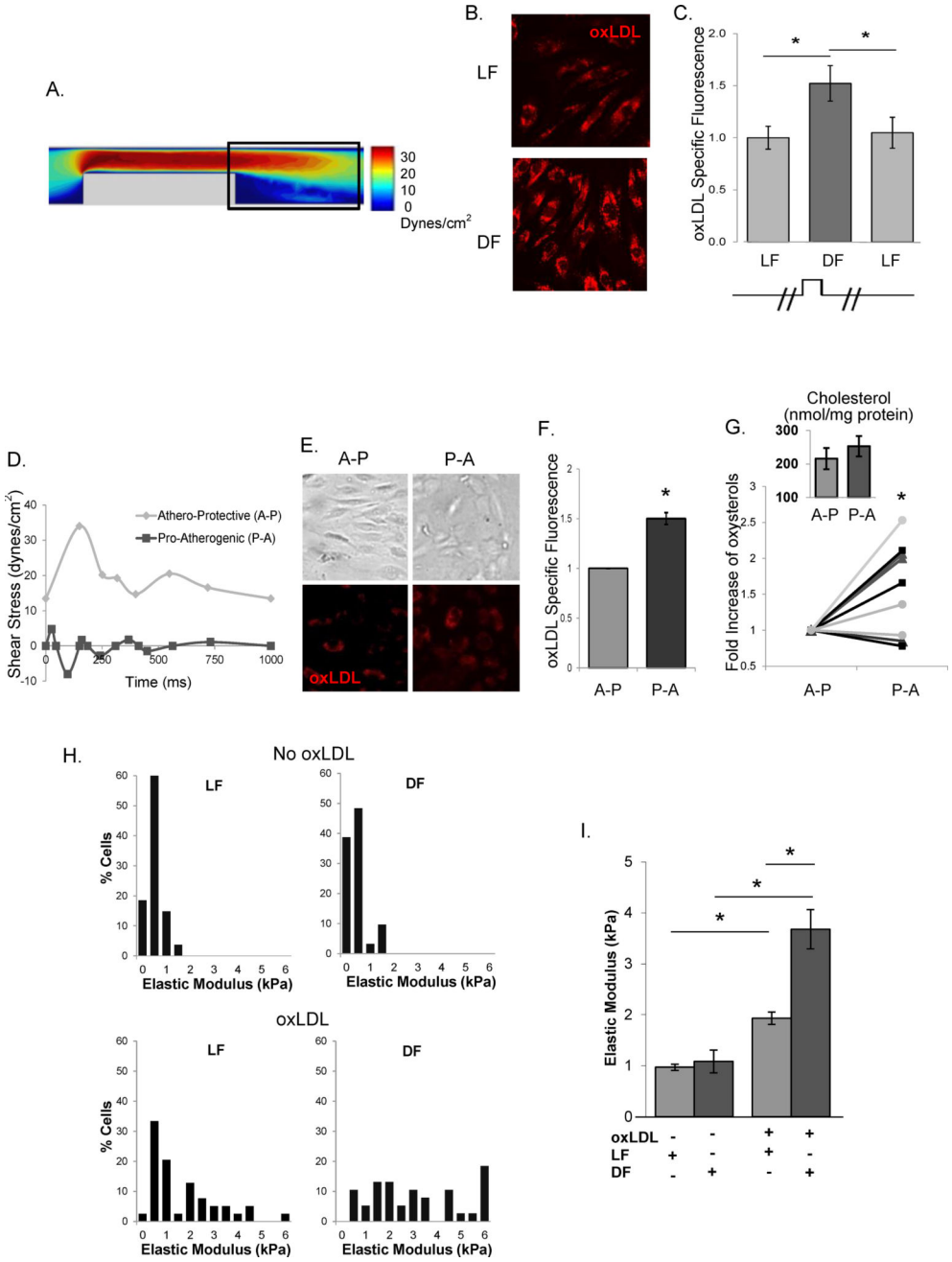

Figure 2. Differential effects of laminar and disturbed flow on oxLDL uptake and oxLDL-induced endothelial stiffening

A: Shear stress values in the side view of the microfluidic chamber obtained by computational fluid dynamic simulation. ***B:*** Representative images of DiI-oxLDL uptake into HAECs under LF and DF. ***C:*** Average oxLDL uptake into HAECs before the step (LF) and after the step (DF, LF) (30–50 cells per condition per experiment, n=6 independent experiments). ***D:*** The athero-protective (A-P) and pro-atherogenic (P-A) flow waveforms used. ***E and F:*** Representative images and average DiI-oxLDL uptake into HAECs under A-P and P-A flows (20–30 cells per condition per experiment, n=4 independent experiments).

G: Quantification of oxysterol (7-ketocholesterol, grey triangles; 5α,6α-epoxycholestanol, black squares; 27-OH-cholesterol, grey circles) and cholesterol (inset) content of ECs under A-P versus P-A flows in the presence of oxLDL using mass spectrometric analysis (n=4). ***H and I:*** Histograms and average elastic modulus values of HAECs in LF and DF regions in the absence or presence of oxLDL (30–60 cells per condition in 3 experiments). *$p<0.05$

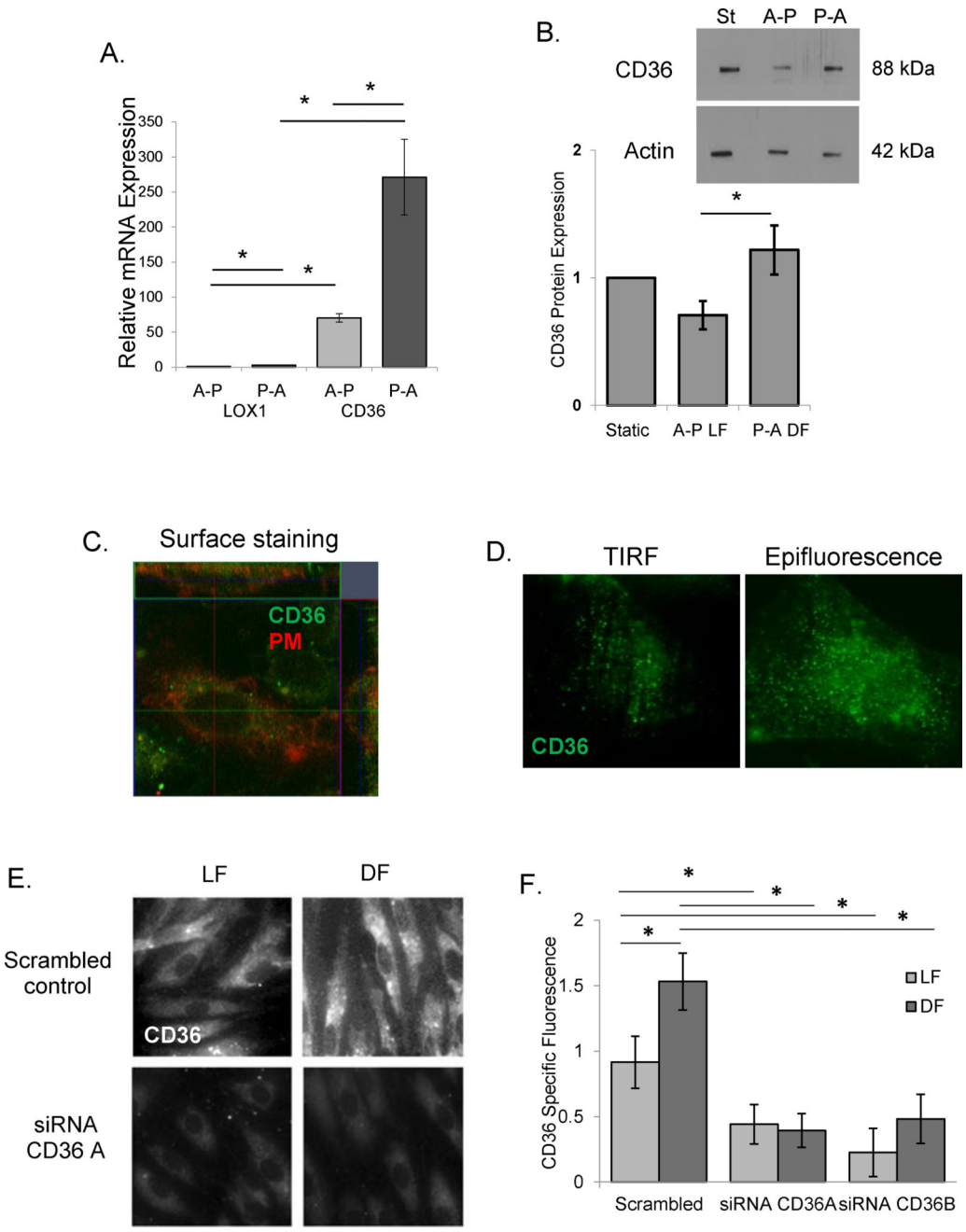

Figure 3. CD36 expression is increased in disturbed flow regions

A and B: Lox1 and CD36 mRNA ***(A)*** and CD36 protein ***(B)*** expression in HAECs exposed to A-P and P-A flows (n=4–6). ***C:*** Representative z-stack confocal image (x-y image, middle; x-z image, top; y-z image, right) of CD36 (green) co-localizing with the plasma membrane (PM, red). ***D:*** HAEC CD36 expression in the basal membrane (TIRF, left) and in the whole cell (epifluorescence, right). ***E and F:*** Representative images of ***(E)*** and average CD36 specific fluorescence ***(F)*** in HAECs exposed to LF and DF, scrambled siRNA and CD36-targeting siRNAs (30–50 cells per experiment; n=3–5 experiments). *p<0.05.

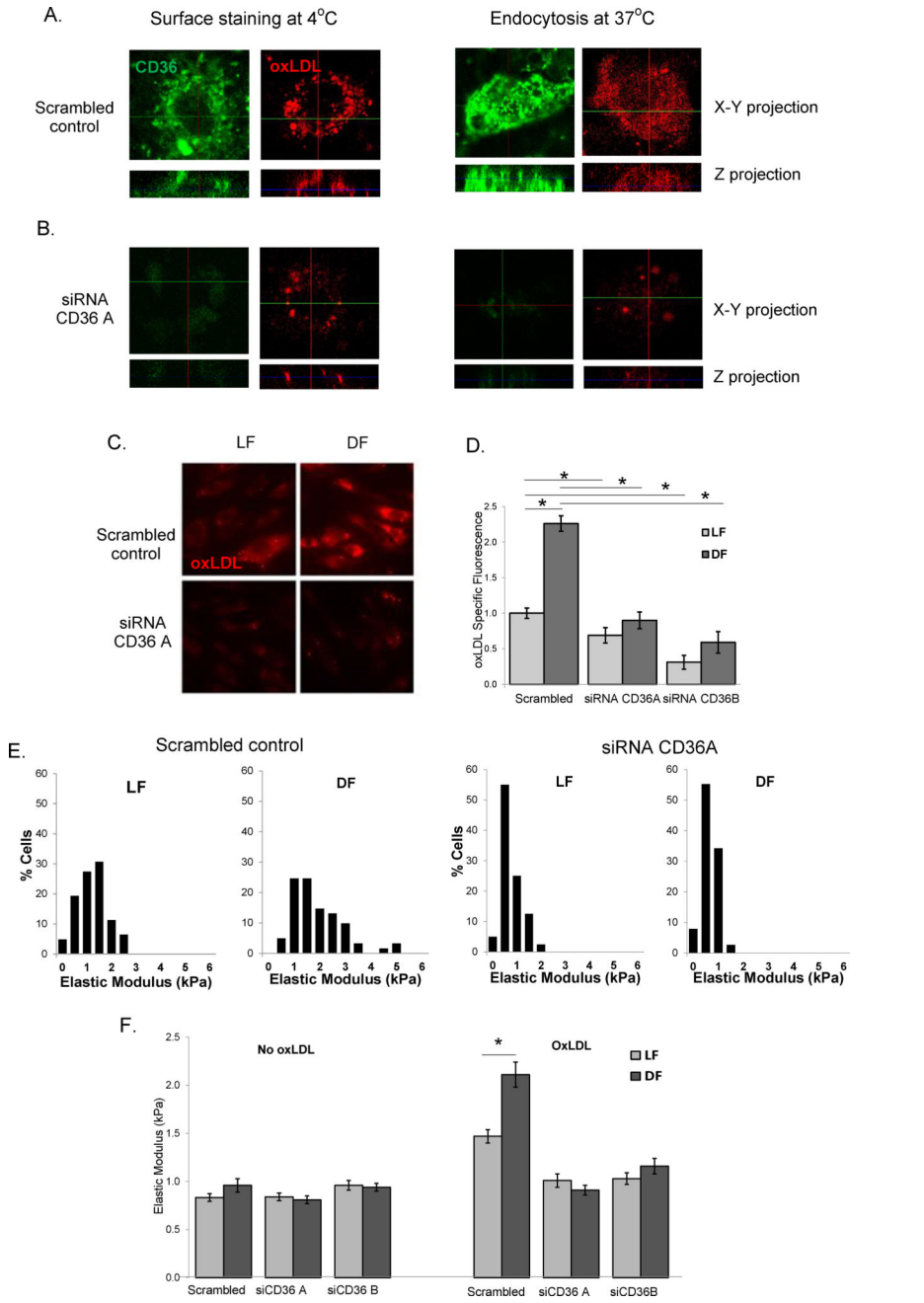

Figure 4. OxLDL uptake and endothelial stiffening is mediated by CD36

A and B: Representative confocal z-stack images (x–y projection, top and z-projection, bottom) of DiI-oxLDL cell surface binding (at 4°C, left) and endocytosis (at 37°C, right) in scrambled control ***(A)*** and CD36-targeting siRNA treated HAECs ***(B)*** (n=3). ***C and D:*** Representative images of ***(C)*** and average ***(D)*** DiI-oxLDL uptake into HAECs exposed to LF or DF, transfected with scrambled or CD36-targeting siRNAs (15–20 cells for each condition per experiment, n=4 experiments). ***E:*** Histograms of the elastic modulus of scrambled and CD36 siRNA_A –treated HAECs exposed to LF or DF in the presence of oxLDL (10–20 cells per condition/experiment; n=3–4). ***F:*** Average elastic moduli for

HAECs exposed to LF or DF in the presence or absence of oxLDL, either with or without CD36-targetting siRNA. *p<0.05.

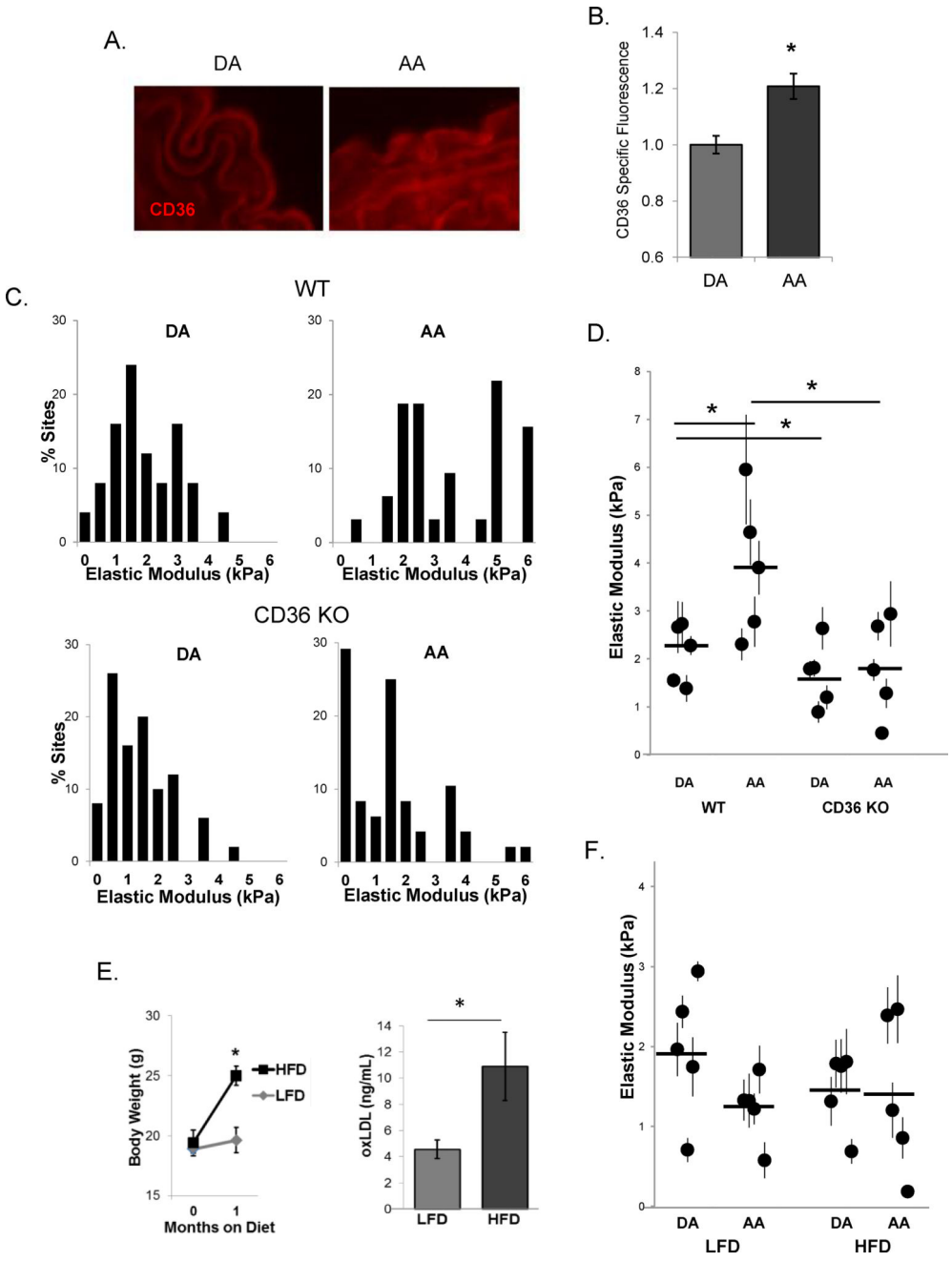

Figure 5. Endothelial stiffening in the aortic arch critically depends on CD36 expression even with high fat diet

A: Representative images of sectioned DA (left) and AA (right) immunostained for CD36. ***B:*** Average CD36 specific staining in mouse aortas (n=3, 3–4 sections per mouse). ***C:*** Histograms of endothelial elastic modulus in the DA and AA regions in 5–6 month old WT and CD36 KO male mice. ***D:*** Average elastic modulus for the DA and AA regions from WT and CD36 KO mice. ***E:*** Average body weights (left, n=7–10 mice) and oxLDL plasma levels (right, n=6 mice) in LFD versus HFD fed mice. ***F:*** Average elastic modulus values for the DA and AA regions from LFD and HFD fed CD36 KO mice. For all mice, 6–10 sites (50–90 AFM measurements) were measured per sample, n=5 mice per condition. *p<0.05.

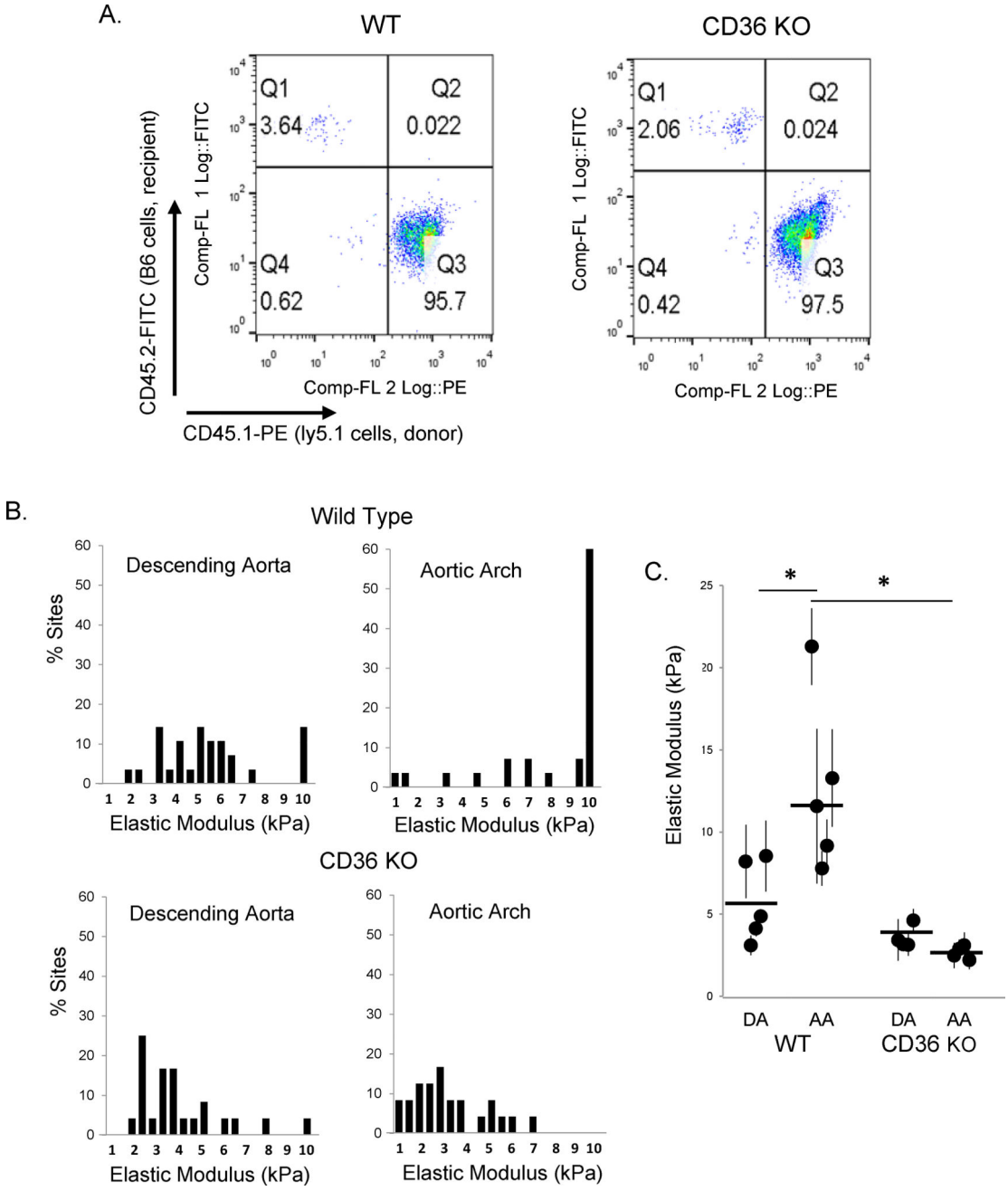

Figure 6. Endothelial softening in the aortic arch of CD36 KO mice is not a "trans" effect of CD36 loss in circulating cells

A: Representative flow cytometry plots depicting bone marrow transfer (BMT) of donor WT macrophages into WT recipients (95.7% transfer, left) and CD36 KO recipient mice (97.5% transfer, right). ***B:*** Histograms of the elastic modulus for the DA and AA regions from WT and CD36 KO BMT mice. ***C:*** Average elastic modulus for the DA and AA from WT and CD36 KO mice two months after irradiation and BMT of donor WT macrophages (6–8 sites [50–70 measurements] per sample, n=4–5 mice per condition). * $p < 0.05$.